

# ANTIPROTON ABSORPTION IN NUCLEI

Yu.T.Kiselev\*

*Institute for Theoretical and Experimental Physics, Moscow, Russia*

E.Ya.Paryev

*Institute for Nuclear Research, Russian Academy of Sciences, Moscow, Russia*

(Dated: April 30, 2018)

We present the analysis of experimental data on forward antiproton production on nuclei. The calculations are done in the framework of a folding model which takes properly into account both incoherent direct proton-nucleon and cascade pion-nucleon antiproton production processes as well as internal nucleon momentum distribution. The effective antiproton-nucleon cross section in nuclear matter and the imaginary part of the antiproton nuclear optical potential are estimated to be 25 – 45 mb and  $-(38 - 56)$  MeV at normal nuclear matter density, respectively. The results of the performed analysis evidence for the decreasing of antiproton absorption in the nuclear medium.

PACS numbers: 25.75 Tw, 25.45.-z, 25.40.-h

## I. INTRODUCTION

The modification of the hadron properties and interactions in baryon environment is one of the important topics of contemporary strong interaction physics. Such a modification has been predicted within various theoretical approaches such as QCD sum rules [1], chiral dynamics [2], relativistic mean-field [3] and quark-meson coupling models [4]. Embedding a hadron in nuclear matter can cause a change of its mass and width. An evidence for a decrease of the  $\rho$  meson in-medium mass in heavy-ion collisions was obtained by the CERES collaboration at CERN [5] and later indicated by the STAR experiment at RHIC [6]. Very recently, the CBELSA/TAPS collaboration reported on the first observation of sizable lowering of the  $\omega$  meson mass at normal nuclear matter density in the  $\gamma Nb$  reaction [7].

The interaction of a hadron in nuclear medium is expected to be also modified leading, in particular, to change of its absorption in nucleus. The results of recent experiment [8] on the  $\phi$  meson photo-production from different nuclei evidence for significant enhancement of the  $\phi$  – nucleon cross section in the nuclear environment. The study of the propagation of antiprotons in nuclear matter can provide the valuable information on the in-medium modification of the  $\bar{p}$  – nucleon interaction.

Anomalous weak absorption of the antiprotons produced in proton-nucleus collisions had been first observed in [9] and then was confirmed in [10, 11]. The inclusive and semi-inclusive  $\bar{p}$  production in  $p\text{Be}$ ,  $p\text{Cu}$  and  $p\text{Au}$  interactions was studied at AGS energies of 12.3 and 17.5 GeV [12]. The analysis within the Glauber-type multiple scattering model performed in [12] shown that the  $\bar{p}$  absorption cross section is at least a factor of 5 smaller than the free  $\bar{p}N$  annihilation cross section. Several mechanisms for the decreased  $\bar{p}$  absorption have

been proposed including finite antiproton formation time [9, 12, 13], "shielding" of the absorption process [14], strong reduction of the phase space available for annihilation due to drop of in-medium  $\bar{p}$  and nucleon masses [15], the formation of  $\bar{p}p$  bound state [16], which was apparently observed in [17]. All of such arguments manifest themselves as a suppression of the antiproton annihilation with nuclear nucleons. Proton-nucleus collisions provide a suitable tool for disentangling of the suggested theoretical schemes and elucidating the dynamics of in-medium antiproton production and absorption in nuclear environment. Using the nuclei as an absorbers has an advantage to have a well defined, nearly static density profile. In this work we present the analysis of inclusive antiproton production in proton-nucleus collisions aimed at the evaluation of the effective antiproton-nucleon cross section in nuclear matter and the imaginary part of the  $\bar{p}$  - nuclear potential.

## II. EXPERIMENTAL DATA

Recently, the differential cross sections for antiproton production on Be, Al, Cu and Ta targets were measured at 10 GeV ITEP synchrotron [18]. The data were taken at initial kinetic proton energies of 5.5, 7.2 and 9.2 GeV. Secondary antiprotons in the momentum range 0.73 – 2.47 GeV/c were detected at  $10.5^\circ$  (lab).

For the evaluation of the antiproton absorption in nuclear matter we use the subset of the experimental data which includes 20 values of the measured differential cross sections on Cu and Ta targets at projectile energies of 7.2 and 9.2 GeV. The reasons for that are the following. First, evidently that the absorption effect is most important for middle and heavy nuclei. Second, it is known that the hadron production in proton-induced reactions at near threshold energies can be described as a superposition of individual collisions of the projectile protons and secondary pions with target nucleons, participating in the Fermi motion. In such a case the elemen-

---

\*Electronic address: yurikis@itep.ru

tary hadron production can be described by the phase space calculations normalized by the corresponding total cross sections. The experimental information about the behavior of the total cross sections for antiproton production in the elementary  $pN$  and  $\pi N$  collisions is available at the excess of collision energy  $\Delta = \sqrt{S} - \sqrt{S_0} \geq 1$  GeV above the corresponding thresholds. The main contribution to the cross section for antiproton production on nuclei comes from the range of  $\Delta > 0.5$  GeV at initial proton energy of 7.2 GeV and from  $\Delta > 0.8$  GeV at 9.2 GeV which are close to the experimentally studied range of  $\Delta$ . That ensures the rather reliable using of the elementary  $\bar{p}$  production cross sections from [19, 20] in our calculations of antiproton creation on nuclei at beam energies of 7.2 and 9.2 GeV. Third, according to the study [20], the influence of the real part of the  $\bar{p}$ -nuclear optical potential on the subthreshold antiproton production in  $pA$  collisions diminishes gradually with increasing bombarding energy and becomes insignificant already at threshold energy of 5.6 GeV. Finally, at above threshold energies the internal nucleon momentum distribution can be safely used instead of the nucleon spectral func-

tion which simplifies the calculations of  $\bar{p}$  production in  $pA$ -reactions.

### III. FOLDING MODEL

The obtained data were analyzed in the framework of the folding model [see [21] for details] accounting for the elementary processes which have the lowest free production thresholds. In addition to the direct antiproton creation via the first chance inelastic proton-nucleon collision,  $p + N \rightarrow \bar{p} + X$ , it is also possible to produce  $\bar{p}$  in two-step cascade process  $p + N \rightarrow N + N + \pi$  followed by  $\pi + N \rightarrow \bar{p} + X$ . Although the threshold for the latter is lower, only high momentum pions contribute to the cross section.

The invariant inclusive cross section for the production on nucleus with atomic mass  $A$  at small laboratory angles an antiproton with the total energy  $E_{\bar{p}}$  and momentum  $\vec{P}_{\bar{p}}$  via the direct reaction channel can be represented as follows:

$$E_{\bar{p}} \frac{d\sigma_{pA \rightarrow \bar{p}X}^{dir}(\vec{P}_0)}{d\vec{P}_{\bar{p}}} = \left\{ 2\pi A \int_0^\infty b db \int_{-\infty}^\infty dz \rho(\sqrt{z^2 + b^2}) \exp \left( -\sigma_{pN}^{in} A \int_{-\infty}^z \rho(\sqrt{b^2 + x^2}) dx - \sigma_{\bar{p}N}^{eff} A \int_z^\infty \rho(\sqrt{b^2 + x^2}) dx \right) \right\} \times \left\{ \int d\vec{q} n(\vec{q}) E_{\bar{p}} \frac{d\sigma_{pN \rightarrow \bar{p}X}(\sqrt{S}, \vec{P}_{\bar{p}})}{d\vec{P}_{\bar{p}}} \right\}. \quad (1)$$

The expression in the first braces describes the distortion of the incident proton and the absorption of the outgoing antiproton in its way out of nucleus. Here  $b$  and  $z$  stand for the impact parameter and the  $z$ -component of the coordinate along the beam axis, respectively. We use  $\sigma_{pN}^{in} = 30$  mb for both considered projectile proton energies which is assumed to be the same for the pp- and pn-collisions. In Eq. (1)  $\sigma_{\bar{p}N}^{eff}$  stands for the effective in-medium antiproton-nucleon cross section. Any difference between the antiproton absorption on nuclear protons and neutrons is disregarded.

In the calculation of  $\bar{p}$  production on Cu and Ta targets we use for the density  $\rho(\vec{r})$  the two-parameter Fermi distribution normalized to unity with parameters  $R=4.20$  fm (Cu),  $R=6.16$  fm (Ta),  $a=0.55$  fm for both nuclei and a nuclear saturation density  $\rho_0=0.17$   $fm^{-3}$ .

The expression in the second braces connects the cross section for  $\bar{p}$  production in the collision of incident proton with off-shell struck target nucleon to the elementary on-shell cross section.

The total energy  $\omega$  of the struck nucleon is related to

its momentum  $\vec{q}$  as follows:

$$\omega = m - \frac{\vec{q}^2}{2M_{A-1}} - \epsilon, \quad (2)$$

where  $m$  and  $M_{A-1}$  stand for free nucleon mass and the mass of the recoiling target nucleus in its ground state, respectively. The nucleon binding energy  $\epsilon$  is taken equal to 6 MeV.

The invariant collision energy squared is read:

$$S = (E_0 + \omega)^2 - (\vec{P}_0 + \vec{q})^2, \quad (3)$$

where  $E_0$  and  $\vec{P}_0$  are total energy and momentum of the projectile proton, respectively.

The internal nucleon momentum distributions  $n(\vec{q})$  in the target nuclei are assumed to be in the form:

$$n(\vec{q}) = \frac{1}{(2\pi)^{3/2}(1+h)} \times \left[ \frac{1}{\sigma_1^3} \exp\left(\frac{-\vec{q}^2}{2\sigma_1^2}\right) + \frac{h}{\sigma_2^3} \exp\left(\frac{-\vec{q}^2}{2\sigma_2^2}\right) \right] \quad (4)$$

with parameters  $h$ ,  $\sigma_1$  and  $\sigma_2$  derived from the data on proton-induced subthreshold and near threshold  $K^+$  pro-

duction on the same set of nuclear targets [22]. The second term in the square brackets represents the high momentum component of the internal nucleon momentum distributions  $n(\vec{q})$  which plays a minor role at considered incident proton energies of 7.2 and 9.2 GeV.

As was above mentioned, in our approach the invariant inclusive cross section for antiproton production in the elementary  $p + N \rightarrow \bar{p} + X$  reaction has been described by the four-body phase space calculations normalized to the corresponding total cross section:

$$E_{\bar{p}} \frac{d\sigma_{pN \rightarrow \bar{p}X}(\sqrt{S}, \vec{P}_{\bar{p}})}{d\vec{P}_{\bar{p}}} = \sigma_{pN \rightarrow \bar{p}X}^{tot}(\sqrt{S}) \frac{R_3(S_{NNN}, m, m, m)}{2R_4(S, m_{\bar{p}}, m, m, m)}. \quad (5)$$

Here  $R_3$  and  $R_4$  are three-body and four-body phase spaces of the reaction  $p + N \rightarrow \bar{p} + N + N + N$ , while  $S_{NNN}$  denotes the invariant energy squared of the not detectable three-nucleon system.

The invariant inclusive cross section for the antiproton production on nucleus A at small laboratory angles via the pion induced reaction channel can be represented as follows [21]:

$$E_{\bar{p}} \frac{d\sigma_{pA \rightarrow \bar{p}X}^{casc}(\vec{P}_0)}{d\vec{P}_{\bar{p}}} = \frac{I_V[A, \sigma_{pN}^{in}, \sigma_{\pi N}^{tot}, \sigma_{\bar{p}N}^{eff}, 0^\circ]}{I'_V[A, \sigma_{pN}^{in}, \sigma_{\pi N}^{tot}, 0^\circ]} \times \sum_{\pi^+, \pi^-, \pi^0} \int d\left(\frac{\vec{P}_\pi}{P_\pi}\right) \int P_\pi^2 dP_\pi \frac{d\sigma_{pA \rightarrow \pi X}(P_\pi)}{d\vec{P}_\pi} \int d\vec{q} n(\vec{q}) \langle E_{\bar{p}} \frac{d\sigma_{\pi N \rightarrow \bar{p}X}(\sqrt{S_\pi}, \vec{P}_{\bar{p}})}{d\vec{P}_{\bar{p}}} \rangle. \quad (6)$$

The first factor in Eq. 6 represents the ratio of the survival probability of an antiproton ( $I_V$ ) to that of a

pion ( $I'_V$ ):

$$I_V = 2\pi A^2 \int_0^\infty b db \int_{-\infty}^\infty dz \rho(\sqrt{b^2 + z^2}) \int_0^\infty dl \rho(\sqrt{b^2 + (z+l)^2}) \exp\left[-\sigma_{pN}^{in} A \int_{-\infty}^z \rho(\sqrt{b^2 + x^2}) dx - \sigma_{\pi N}^{tot} A \int_z^{z+l} \rho(\sqrt{b^2 + x^2}) dx - \sigma_{\bar{p}N}^{eff} A \int_{z+l}^\infty \rho(\sqrt{b^2 + x^2}) dx\right]$$

$$I'_V = 2\pi A \int_0^\infty b db \int_{-\infty}^\infty dz \rho(\sqrt{b^2 + z^2}) \exp\left[-\sigma_{pN}^{in} A \int_{-\infty}^z \rho(\sqrt{b^2 + x^2}) dx - \sigma_{\pi N}^{tot} A \int_z^\infty \rho(\sqrt{b^2 + x^2}) dx\right]. \quad (7)$$

In the following calculations  $\sigma_{\pi N}^{tot} = 35$  mb for all pion momenta.

The expression for the cross section for  $\bar{p}$  production in the elementary  $\pi N$  collisions has the form similar to that for proton-induced reaction:

$$\langle E_{\bar{p}} \frac{d\sigma_{\pi N \rightarrow \bar{p}X}(\sqrt{S_\pi}, \vec{P}_{\bar{p}})}{d\vec{P}_{\bar{p}}} \rangle = \frac{Z}{A} E_{\bar{p}} \frac{d\sigma_{\pi p \rightarrow \bar{p}X}(\sqrt{S_\pi}, \vec{P}_{\bar{p}})}{d\vec{P}_{\bar{p}}} + \frac{A-Z}{A} E_{\bar{p}} \frac{d\sigma_{\pi n \rightarrow \bar{p}X}(\sqrt{S_\pi}, \vec{P}_{\bar{p}})}{d\vec{P}_{\bar{p}}}, \quad (8)$$

where Z stands for the atomic weight of the nucleus and

$$E_{\bar{p}} \frac{d\sigma_{\pi N \rightarrow \bar{p}X}(\sqrt{S_\pi}, \vec{P}_{\bar{p}})}{d\vec{P}_{\bar{p}}} = \frac{\pi}{4} \sigma_{\pi N \rightarrow \bar{p}X}^{tot}(\sqrt{S_\pi}) \frac{\sqrt{S_{NN} - 4m^2}}{R_3(S_\pi, m_{\bar{p}}, m, m) \sqrt{S_{NN}}}. \quad (9)$$

Here  $R_3$  is the three-body phase space of the reaction  $\pi + N \rightarrow \bar{p} + N + N$ , while  $S_{NN}$  denotes the invariant energy squared of the not detectable two-nucleon system. In case of pion-induced antiproton production the invariant

collision energy squared is read:

$$S_\pi = (E_\pi + \omega)^2 - (\vec{P}_\pi + \vec{q})^2, \quad (10)$$

where  $E_\pi$  and  $\vec{P}_\pi$  are the pion total energy and momentum, respectively.

The elementary  $\bar{p}$  production processes  $\pi^+n \rightarrow p\bar{p}p$ ,  $\pi^0n \rightarrow p\bar{p}n$ ,  $\pi^0p \rightarrow p\bar{p}p$ ,  $\pi^-p \rightarrow p\bar{p}n$  and  $\pi^-n \rightarrow n\bar{p}n$  have been included in our calculations of the  $\bar{p}$  creation on nuclei of interest.

The differential cross sections for pion production by protons on nuclear targets were deduced from data [10, 23, 24]. High momentum part of the pion spectra is approximated in the form:

$$E_\pi \frac{d\sigma_{pA \rightarrow \pi X}(\vec{P}_\pi)}{d\vec{P}_\pi} = A(1 - X_F^R)^{B - (X_F^R)^2 + CP_\perp^2} [mb \text{ GeV}^{-2} c^3 \text{ sr}^{-1}] \quad (11)$$

with constants A, B, C listed in Table I. In Eq.(11) the radial scaling variable  $X_F^R$  is given by

$$X_F^R = \frac{\sqrt{P_l^{*2} + P_\perp^2}}{P_{max}^*}, \quad (12)$$

where  $P_l^*$  and  $P_\perp$  are the longitudinal and transverse momenta of pion in the pA center-of-mass system, respectively;  $P_{max}^*$  is the maximum value of  $P^*$  allowed by the kinematics. The expression (11) reproduces all available data on small angle pion production in proton-nucleus collisions in the projectile energy range from 5 to 24 GeV within the accuracy of about 25 %. The  $\pi^0$  spectrum also needed for the calculations can be approximately expressed as an arithmetic mean of the  $\pi^+$  and  $\pi^-$  spectra.

TABLE I: Coefficients A, B, C of Eq.(11)

	Cu			Ta		
	A	B	C	A	B	C
$\pi^+$	700	3.7	4.0	1000	3.8	4.2
$\pi^-$	380	4.2	4.7	650	3.9	4.5

#### IV. DATA ANALYSIS

For the present analysis the antiproton production in the elementary  $pN$  and  $\pi N$  collisions as well as the final antiproton absorption in its way out of the nucleus are of relevance. The parametrization of the total cross section for both production channels is based on the results [19, 20] obtained within the One-Boson-Exchange model:

$$\sigma_{hN \rightarrow \bar{p}X}^{tot} = a(S/S_0 - 1)^b (S/S_0)^c. \quad (13)$$

Here  $\sqrt{S}$  stands for the invariant collision energy, while  $\sqrt{S_0}$  denotes the threshold for the individual channel

given by the sum of the hadron masses in the final state of the reaction. The values of the parameters  $a$ ,  $b$ ,  $c$ , used in the following calculations, are listed in Table II. The analysis [19, 20] indicates a phase space dominance for the antiproton production cross sections both from pion and nucleon induced reactions.

TABLE II: The parameters in the approximation (13)

Reaction	$S_0$	$a$ , mb	$b$	$c$
$\pi N \rightarrow \bar{p}X$	9 $m^2$	1	2.31	-2.3
$pN \rightarrow \bar{p}X$	16 $m^2$	0.12	3.5	-2.7

The calculations by Eqs. (1) - (13), employing a phase space behavior of the total  $\bar{p}$  production cross sections (Table II) and a free inelastic  $\bar{p}N$  cross section [25] as an effective in-medium antiproton-nucleon cross section  $\sigma_{\bar{p}N}^{eff}$ , essentially fail in describing the experimental data on Cu and Ta target nuclei. The mean value of the ratio of the calculated and measured antiproton production cross sections is equal to about 0.4.

Thus, in the next calculation we assume that for both antiproton production channels the total elementary  $\bar{p}$  production cross sections follow the available phase space and treat  $\sigma_{\bar{p}N}^{eff}$  as a free parameter. It is found that the experimental data can be reasonably reproduced by the calculation implying  $\sigma_{\bar{p}N}^{eff} = 35$  mb for all considered antiproton momenta (Fig.1). The uncertainty in the effective in-medium antiproton-nucleon cross section caused by experimental errors is estimated to be  $\pm 10$  mb.

The calculations by Eqs (1) - (13) provide the possibility to study the relative contributions of the direct and cascade antiproton production mechanisms. It is found that the strengths of these competing production channels slightly depend on the effective in-medium  $\bar{p}N$  cross section. The contribution of the direct channel to the antiproton production cross section at projectile proton energy of 7.2 GeV, defined as a ratio  $R = (\frac{E}{P^2} \frac{d^2\sigma}{dP d\Omega})^{dir} / [(\frac{E}{P^2} \frac{d^2\sigma}{dP d\Omega})^{dir} + (\frac{E}{P^2} \frac{d^2\sigma}{dP d\Omega})^{casc}]$ , is shown in Fig.2 for Cu and Ta targets. One can see that the role of the direct mechanism increases with antiproton momentum while the role of the cascade mechanism decreases as more energetic pions are required to produce fast antiproton. Since the cascade mechanism probes more dense layers of the nucleus the knowledge of these contributions is required for the estimate of the nuclear density involved in the  $\bar{p}$  production.

Furthermore, it is well known that in the optical model the particle absorption in nucleus is connected with the imaginary part of the respective nuclear optical potential, which provides the possibility to evaluate its magnitude.

The propagation through the nuclear matter of the  $\phi$  mesons produced in  $\gamma A$  [26] and  $pA$  [27, 28] reactions has been studied within the Glauber type scattering model. The change in the  $\phi$  absorption was attributed to the modification of its width in nuclear medium. Following the receipt of Ref. [27] we express the antiproton survival

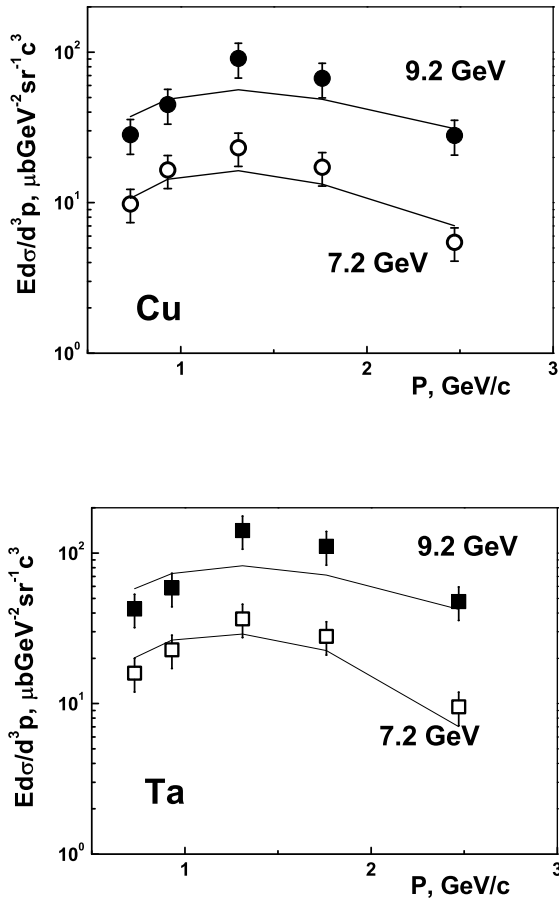


FIG. 1: Invariant cross sections for antiproton production in  $pCu$  and  $pTa$  interactions at initial proton energies of 7.2 and 9.2 GeV as a function of  $\bar{p}$  momentum. The experimental data are from [18]. The curves are our calculations with  $\sigma_{\bar{p}N}^{eff} = 35mb$

probability in the form:

$$W = \exp\left(\int_z^\infty dx Im\Pi(P_{\bar{p}}, \rho(r'))/P_{\bar{p}}\right). \quad (14)$$

Here  $\Pi(P_{\bar{p}}, \rho(r'))$  be the antiproton self-energy in a nuclear medium as a function of its momentum  $P_{\bar{p}}$  and the nuclear density  $\rho(r')$  with the antiproton production point inside the nucleus  $r' = \sqrt{b^2 + x^2}$ .

Since the nuclear optical potential  $U = \Pi(P_{\bar{p}}, \rho)/2E_{\bar{p}}$ , Eq. (14) can be rewritten as:

$$W = \exp\left(2 \int_z^\infty dx ImU(P_{\bar{p}}, \rho(r'))/\beta\right). \quad (15)$$

where  $\beta = P_{\bar{p}}/E_{\bar{p}}$  stands for  $\bar{p}$  velocity in the target nucleus frame of reference.

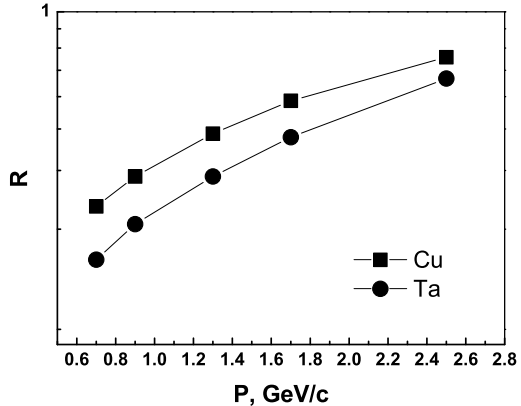


FIG. 2: Contribution of the direct channel to the antiproton production cross section at incident proton energy of 7.2 GeV as a function of  $\bar{p}$  momentum.

On the other hand, this probability in Eq.(1) and Eq.(7) is read as:

$$W = \exp\left(-\int_z^\infty dx \sigma_{\bar{p}N}^{eff} \rho(r')\right). \quad (16)$$

From the comparison of Eq.(15) and Eq.(16) one gets the expression for the imaginary part of the antiproton optical potential in the nuclear matter:

$$ImU = -\beta \sigma_{\bar{p}N}^{eff} \rho(r')/2. \quad (17)$$

Now we can evaluate the  $ImU$  at an estimated average nuclear density involved  $\rho = 0.36\rho_0$  assuming the mean value of the  $\sigma_{\bar{p}N}^{eff} = 35$  mb. The imaginary part of the antiproton optical potential changes from -14 MeV at antiproton momentum of 0.73 GeV/c till -20 MeV at 2.5 GeV/c due to its dependence on the antiproton velocity  $\beta$ . Thus, the magnitude of  $ImU$  can be estimated as  $-(38 - 56)$  MeV at  $\rho = \rho_0$ . These values are sizably larger than the imaginary part of the antiproton nuclear optical potential derived from the analysis of data on antiprotonic atoms [29] which is close to -160 MeV. However, in [29] the optical potential is determined at radii where density is  $(0.02 - 0.03)\rho_0$  and the extrapolation of this potential to the central nuclear density is highly model dependent. Note that our estimate of the imaginary part of  $\bar{p}$ -nuclear potential is comparable with the magnitudes of  $ImU$  calculated for the  $\phi$  mesons [26, 27] as well as for the antikaons [30].

## V. CONCLUSION

The analysis of the data on antiproton production on Cu and Ta nuclei within the folding model, including

proton- and pion-induced production channels, evidences for the effective in-medium  $\bar{p}N$  cross section in the momentum range 0.7-2.5 GeV/c is within (25–45) mb. This value differs from free total and inelastic  $\bar{p}N$  cross sections, which demonstrate strong momentum dependence and significantly larger magnitudes. The imaginary part

of the antiproton nuclear optical potential is estimated to be  $-(38 - 56)$  MeV at normal nuclear matter density.

The authors acknowledge valuable discussions with V.A.Sheinkman and for providing us with experimental data prior to publication.

- 
- [1] T. Hadsuda and S. Lee, Phys.Rev. **C46**, R34 (1992).  
 [2] G. Brown and M. Rho, Phys.Rev.Lett. **66**, 2720 (1992).  
 [3] P. S. Reinhard Rep.Prog.Phys. **52**, 439 (1989).  
 [4] T.Tsushima et al., Phys.Lett. **B429**, 239 (1998).  
 [5] G.Agakichiev et al., Phys.Lett. **B422**, 405 (1998).  
 [6] J.Adams et al., Phys.Rev.Lett. **92**, 092301 (2004).  
 [7] D.Trnka et al., Phys.Rev.Lett. **94**, 192303 (2005).  
 [8] T.Ishikawa et al., Phys.Lett.**B608**, 215 (2005).  
 [9] A.Vaisenberg et al., Pis'ma Zh.Exsp.Teor.Fiz. **29**, 719 (1979).  
 [10] Y.Sugaya et al., Nucl.Phys. **A634**, 115 (1998).  
 [11] T.Abbot et al., Phys.Rev. **C47**, 1351 (1993).  
 [12] I.Chemakin et al., Phys.Rev. **C64**, 064908 (2001).  
 [13] W.Cassing et al., Nucl.Phys. **A707**, 224 (2002).  
 [14] S.Kahana et al., Phys.Rev. **C47**, 1356 (1993).  
 [15] I.N.Mishustin et al., Phys.Rev. **C71**, 03520 (2005).  
 [16] I.S.Shapiro, Phys.Rep. **C35**, 129 (1978).  
 [17] J.Z.Bai et. al., Phys.Rev.Lett. **91**, 022001 (2003).  
 [18] V.A.Sheinkman, private communication; to be submitted to Phys.At.Nucl.  
 [19] G. Lykasov M. Rzjanin and W. Cassing, Phys.Lett. **B387**, 691 (1996).  
 [20] A. Sibirtsev et. al., Nucl. Phys. **A632**, 131 (1998).  
 [21] E. Ya. Paryev, Eur. Phys. J. **A9**, 521 (2000).  
 [22] A. V. Akindinov et. al., JETP Lett. **72**, 100 (2000).  
 [23] T. Eichten et. al., Nucl. Phys. B **44**, 333 (1972).  
 [24] Yu. Bayukov et. al., Sov. J. Nucl. Phys. **29**, 947 (1979).  
 [25] Review of Particle Properties, Phys.Rev. **D50**, 131 (1994).  
 [26] D.Cabrera et. al., Nucl. Phys. **A733**, 130 (2004).  
 [27] V.K.Magas et al., Phys.Rev. **C71**, 065202 (2005).  
 [28] E. Ya. Paryev, Eur. Phys. J **A23**, 453 (2005).  
 [29] E.Friedman et al., Nucl.Phys. **A761**, 283 (2005).  
 [30] A.Ramos, E.Oset, Nucl. Phys. **A671**, 481 (2000).